Optical Engineering

SPIEDigitalLibrary.org/oe

Thermal annealing of laser damage precursors on fused silica surfaces

Nan Shen
Philip E. Miller
Jeff D. Bude
Ted A. Laurence
Tayyab I. Suratwala
William A Steele
Michael D. Feit
Lana L. Wong

SPIE

Thermal annealing of laser damage precursors on fused silica surfaces

Nan Shen
Philip E. Miller
Jeff D. Bude
Ted A. Laurence
Tayyab I. Suratwala
William A Steele
Michael D. Feit
Lana L. Wong
Lawrence Livermore National Laboratory
7000 East Avenue
Livermore, California 94550
E-mail: nshen@llnl.gov

Abstract. Previous studies have identified two significant precursors of laser damage on fused silica surfaces at fluences <35 J/cm^2: photoactive impurities from polishing and surface fractures. We evaluate isothermal heating as a means of remediating the defect structure associated with surface fractures. Vickers indentations are applied to silica surfaces at loads between 0.5 and 10 N, creating fracture networks. The indentations are characterized before and following thermal annealing under various time and temperature conditions using confocal time-resolved photoluminescence (CTP) imaging, and $R/1$ damage testing with 3-ns, 355-nm laser pulses. Improvements in the damage thresholds with reductions in CTP intensity are observed at temperatures well below the glass transition temperature (T_g). The damage threshold on 0.5-N indentations improves from <8 to >35 J/cm^2 after annealing at approximately 750°C. Larger fracture networks require longer or higher temperature treatment to achieve similar results. At an annealing temperature >1100°C, optical microscopy indicates morphological changes in some of the fractures surrounding the indentations, although remnants of the original fractures are still observed. We demonstrate the potential of using isothermal annealing to improve the laser damage resistance of silica optics, and provide a means of further understanding the physics of optical damage and mitigation. [DOI: 10.1117/1.OE.51.12.121817]

Subject terms: annealing; laser-induced damage; fluorescence spectroscopy; fused silica; surfaces.

Paper 120486SSP received Apr. 2, 2012; revised manuscript received Aug. 29, 2012; accepted for publication Sep. 13, 2012; published online Oct. 10, 2012.

1 Introduction

There is a long-standing interest in the use of high average, high-peak power lasers in demanding applications such as inertial confinement fusion (ICF).[1–4] The peak power that can be sustained by such lasers is typically limited by the amount of self-induced damage that can be tolerated by components making up the optical delivery system. All optical materials, including fused silica, have intrinsic absorption properties that will ultimately lead to damage at sufficiently high laser intensities. In practice, however, surface damage at fluences well below the intrinsic limit have limited the performance of even the highest quality optical components.[5,6] These components can absorb photons with energies below the material band gap causing undesirable damage when exposed to high fluence light. A number of studies have focused on indentifying the surface defects which may lead to such optical damage.[7–9] Recent studies[9] suggest that two sources of absorption exist that are primarily responsible for optically induced surface damage of fused silica optics exposed to ultraviolet wavelengths at fluence $< \approx 35$ J/cm^2. These include optical absorption by photoactive impurities and absorption by a thin layer of electronically defective material associated with even minute fractures on silica surfaces.

Moreover, confocal time-resolved photo-luminescence microscopy (CTP) studies demonstrate the spatial coincidence between locations giving rise to a characteristic fast photoluminescent (FPL) signal and the locations where optical damage occurs when subjected to high fluence subband gap laser illumination. This useful diagnostic led us to hypothesize that fracture surfaces generated during indentation processes[10] (including grinding, handling, intense laser irradiation, etc.) create a region rich in defects. The photoluminescence (PL) observed from these fracture defects exhibits a broad distribution of lifetimes typically much shorter (<1 ns) than those observed from isolated point defects known to occur in silica glass, such as oxygen deficiency centers (ODCs) and nonbridging oxygen hole centers (NBOHCs) (approximately 20 μs).[11–13] We hypothesize that the local density of defects is sufficiently high near fracture surfaces so that they interact to form a quasi-continuum of electronic energy states, which results in fast PL and high absorptivity of subband gap light. These states provide a means of transferring enough energy from the optical beam to the glass matrix to cause optical damage.

One widely applied method of removing point defects is to thermally anneal the material in a furnace. Studies of defects induced by irradiation from neutrons or near-infrared femtosecond laser sources have shown that point defects in fused silica start to anneal away at temperatures as low as 300°C, and that the annealing process is accompanied by a significant reduction in PL[14,15] signal. At temperatures of approximately 500°C, the PL characteristic of point defects almost disappears, indicating the reconstruction of broken Si—O generated during the initial irradiation.

Analogously, we have shown that it may be possible to anneal out the defects associated with fractures that form

the quasi-continuum states in fused silica using an isothermal furnace without *a priori* knowledge of the defect locations. This offers the possibility of improving the resistance of fused silica optics to optical surface damage. In this paper, we provide results on isothermal annealing on both the PL characteristics of fused silica, and their corresponding propensity to optical damage.

2 Experiment

Fractures responsible for the subband gap absorption of light in fused silica can originate from optical fabrication steps, such as shaping or polishing operations. Alternately micro-scale fractures may be introduced as simple handling scratches or digs. In the present work we have used a Vickers indenter[16,17] as a reproducible means of producing surface fractures on test specimens. The test substrates used in the present work were 2-in. diameter fused silica windows from CVI-Melles-Griot. Prior to indentation, samples were chemically leached to remove photoactive impurities[18] from the near surface of the optics. Indentation was performed using a Shimadzu Model HVM 2 micro-hardness tester, equipped with a Vickers indenter, using indentation loads ranging between 0.5 and 10 N. Such indentations resulted in the formation of fracture networks approximately 10 to 80 μm in diameter and 1 to 20 μm deep, as shown in Fig. 1. Although not evident by optical microscopy, a more careful secondary electron microscopy (SEM) study revealed that small (approximately 20-nm wide) fractures are present around the periphery of the plastically deformed zone[18] of even the 0.5-N indentations.

In addition to optical and secondary electron microscopy, indentations were characterized both before and after isothermal annealing using CTP imaging to look at the fast component ($\tau < 5$ ns) of the photoluminescence (FPL) signal. This technique has been described in detail elsewhere.[19] Following indentation, samples were isothermally annealed in a furnace under a nitrogen atmosphere to minimize the air oxidation and creation of substoichiometric oxides. The heating and cooling cycle was carefully controlled to minimize the possibility of introducing thermal stress into the glass by using 5°C/ min heating and cooling rates. Using a series of samples, the annealing temperature was varied over a range from 750°C to 1150°C, and the annealing time was varied from 3 to 96 h.

The damage propensity of each sample was assessed using small beam $R/1$ laser damage testing.[20] For optics with randomly distributed damage precursors, damage testing is typically performed using a centimeter-sized beam and reported as damage density as a function of laser fluence $\rho(\phi)$. The test results using small beams, on the other hand, may depend strongly on the beam size. We used small beam $R/1$ damage testing as we are dealing with highly localized damage precursors. Within the indentation fracture network, there is a high density and relatively homogeneous distribution of damage precursors that can be seen in the CTP imaging. During laser irradiation, some of these precursors absorb laser light and initiate damage. The local laser fluence where damage takes place is obtained by cross-registering a laser fluence map with each damage location. A second advantage of small beam damage testing is that one can target specific regions of the sample surface with spatial selectivity.

The small beam laser damage testing in this study was performed using a Coherent Infinity Q-switched Nd:YAG laser operating at 355 nm. The temporal profile of the laser pulse is Gaussian with FWHM pulse duration of approximately 3 ns. The laser is focused onto the indentation on the exit surface of the silica specimen using a long focal distance lens as shown in Fig. 2. The laser pulse energy and its spatial profile are monitored by picking off a fraction of the beam and recording it using a charge coupled device (CCD) camera. The beam has a $1/e^2$ diameter of approximately 80 μm. An imaging microscope is used to observe the sample under laser irradiation. During damage testing, the laser pulse energy is slowly ramped to achieve an approximate 5-J/cm^2 step increase. A single laser pulse is fired at the sample during each fluence step, and the sample is inspected on the imaging camera until damage is registered. Depending on the size of the fracture network (i.e. indentation load), the size of the laser induced damage site ranges from a few to several tens of micrometers. In order to obtain an accurate measurement of the laser fluence, we cross register the laser fluence map with the damage features observed on the sample, and calculate the local fluence of the laser in the locality where each damage event is observed. Between four and ten indentations at each load were tested for each annealing condition. We then calculated the average and standard deviation of the damage fluence associated with each annealing condition.

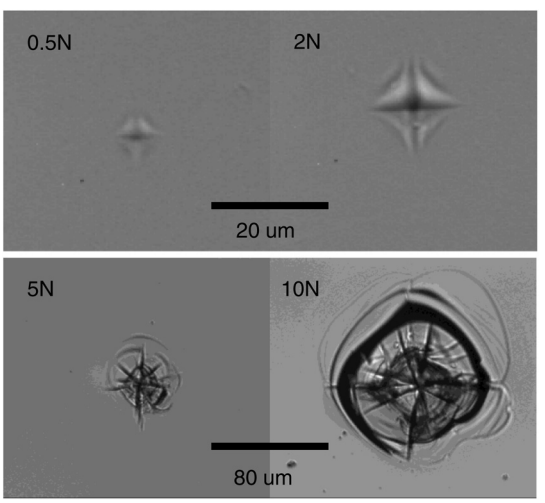

Fig. 1 Optical micrographs of typical Vickers indentations at different loads.

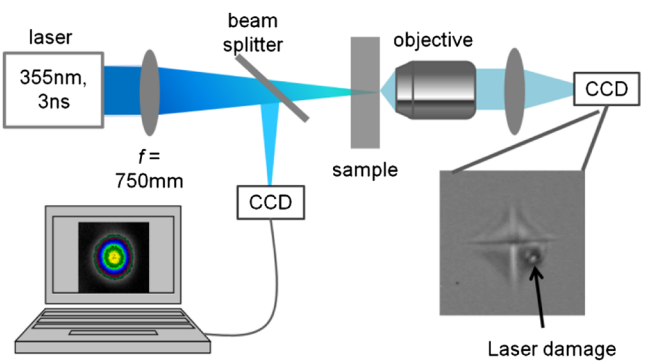

Fig. 2 Schematic diagram of the small beam $R/1$ laser damage system.

3 Results

As one might expect, longer annealing times progressively reduced the FPL signal associated with fracture surfaces [see Fig. 3(a)]. Similarly the damage threshold of the surface exhibited a rapid initial rise as a function of annealing time [Fig. 3(b)]. At longer annealing times, the laser damage threshold was found to plateau to a steady state value. In general, smaller indentations (i.e., smaller fracture networks resulting from lower indentation loads) annealed faster and reached a higher steady state damage threshold than did larger fracture networks originating from larger indentation loads. In the case of 0.5-N indentations, isothermal annealing produced a surface having a damage threshold of approximately 35 J/cm^2. This approaches the threshold of approximately 41 J/cm^2, which corresponds to that of an acid-leached,[21] fracture-free fused silica surface measured using the same small beam $R/1$ method. Indentations created using all three of the loads used in the present time study reached their steady state value within an annealing time of 48 h.

In Fig. 4, the damage initiation threshold, in the vicinity of a series of indentations applied at four different loads, is compared as a function of temperature for a fixed annealing time of 48 h. The annealing temperatures used in the present work ranged between 750°C and 1150°C, and in all cases was kept below the thermal stress relief point (approximately 1200°C) of the bulk glass to minimize potential distortions of the optical surfaces. Representative FPL images of different indentations before and after annealing are shown in Fig. 4(a). A significant reduction in the FPL signal was observed for all the indentations at each temperature. Furthermore, the decreased density of metallic-like defect states, as indicated by the decreases in the FPL image,[8] was also reflected in the laser damage testing results summarized in Fig. 4(b). In particular, the data shown in Fig. 4(b) illustrates the laser damage threshold, following thermal annealing, is a function of both the lateral size of fracture network initially present on the surface of the optic, and the annealing temperature used. Smaller fracture networks, (i.e., fractures formed at lower indentation loads) and higher annealing temperatures typically resulted in higher optical damage thresholds. Since the annealing temperature was kept well below the glass softening point, one would expect a minimal amount of surface modification due to viscous flow. This suggests that the improvement in the damage performance in the vicinity of the indentation is the result of the local reconstruction of the defect layer (e.g., the reorganization of dangling bonds, and thus, a reduction in precursor density) on the surface of the fracture that gives rise to subband gap absorptivity. The extent of the annealing of the fracture induced defects at the temperatures used in the present work is dependent on the extent and severity of the initial

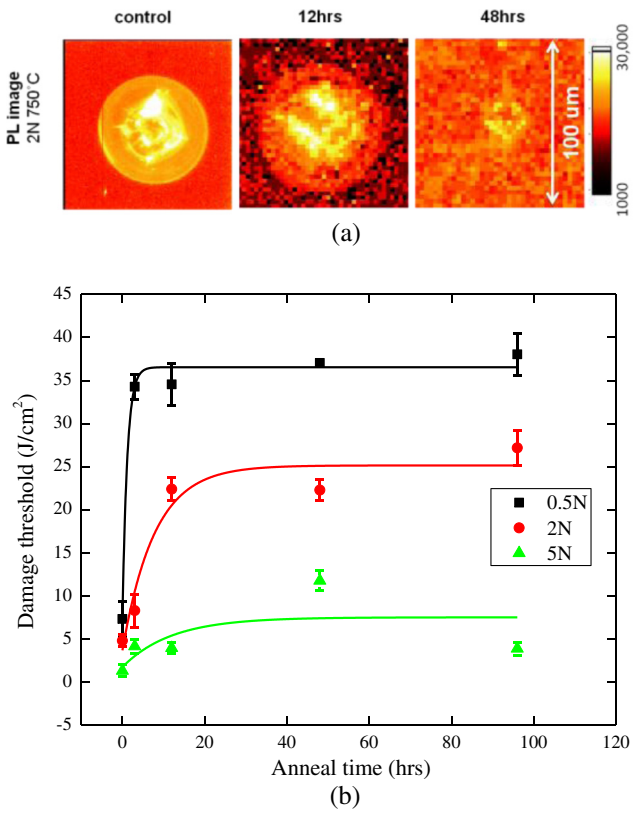

Fig. 3 Time dependent isothermal annealling. (a) Reduction of characteristic fast photoluminescence (PL) as a function of annealing time for a 5-N indentation at 750°C. (b) Damage threshold as a function of annealing time at 750°C. Solid lines are an exponential fit to the data of the form $Y(t) = Y_0 + A\exp(Bt)$ where A and B are the fitting parameters, and t is the annealing time.

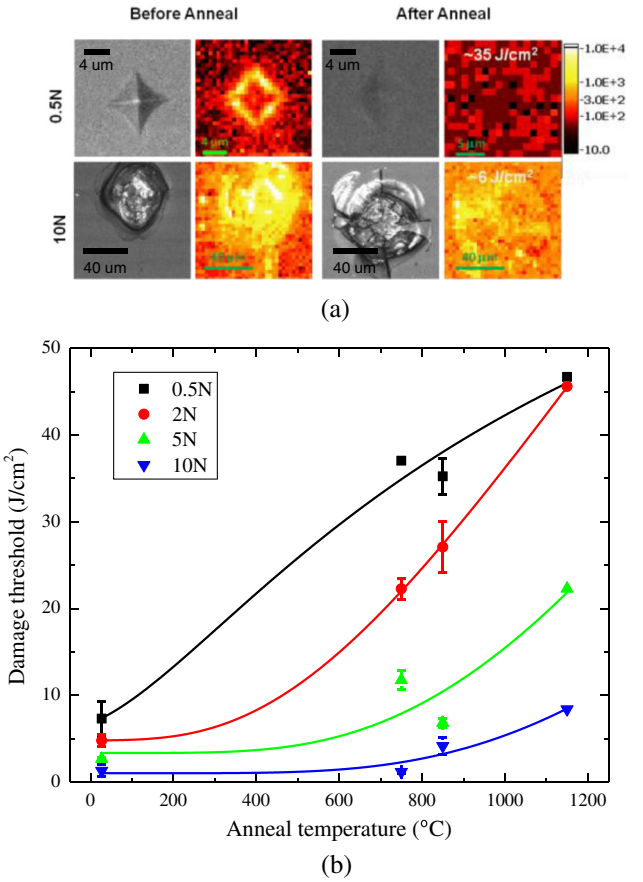

Fig. 4 Temperature dependent isothermal annealing of indentations. (a) Typical fast photoluminescence (PL) images of 0.5 and 10-N indentations prior to and following 48 h of annealing at 1150°C. (b) Damage threshold, determined by $R/1$ damage testing, as a function of annealing temperature for 0.5, 2, 5, and 10-N indentations. Solid lines are Arrhenius fits to the data.

fracture network. A detailed description of the rearrangement of the defect layer or the specific relationship between defect density and damage threshold is beyond the scope of the present paper. However, the present data does suggest that the improvement in the damage threshold associated with the annealing process is a temperature-dependent process, while higher annealing temperatures result in higher damage thresholds, and improvements in the damage threshold can be realized at temperatures well below the glass transition temperature. Moreover, in light of the temperature dependence of the damage threshold improvement, it is not unreasonable to assume that the annealing process is a thermally activated process, which might be expected to follow an Arrhenius law. If we assume the damage threshold associated with each indentation load depends linearly on the precursor density, one might express the damage threshold (F) as a function of the annealing temperature (T):

$$F = F_{\text{room}} + F_0 \exp[-E_a/(RT)], \tag{1}$$

where F_{room} is the damage threshold at room temperature, F_0 is a fitting constant, E_a is the activation energy of the thermally activated annealing process, and R is the gas constant. Table 1 summarizes the fitting parameters for different indentation loads. Because of the limited number of data used in the fit, the uncertainties in the fitting parameters are expected to be large. As reflected in Table 1, one would qualitatively expect higher indentation loads would lead to lower initial damage thresholds (e.g., successively lower values of F_{room}), and progressively larger thermal barriers (e.g., E_a) associated with the annealing of the defect layers. In addition, the pre-exponential factor in the Arrhenius equation, also known as the frequency factor, increases for higher indentation loads as the precursor density increases. Nonetheless, given the small dataset and limited knowledge relative to, for example, the functional relationship between defect density and damage threshold, the Arrhenius fit is meant to be a guide to how precursor density (i.e., indentation load) and annealing temperature qualitatively affect the laser damage threshold.

4 Discussion

A number of physical and mechanical processes occur as a silicate glass is heated. We have attempted to schematically summarize several of these processes in Fig. 5. As shown in this figure, only relatively modest temperatures (approximately 400°C) and times are required to anneal out isolated point defects. As the density of defect states increases, one would expect higher temperatures and/or longer times would be required to reconstruct the high density of defects that result in the formation of the quasi-continuum of electronic states responsible for subband gap absorption. As the temperature is raised further (approximately 1200°C), mechanical stresses in the bulk material are relieved. Further heating results first in softening of the material and eventually in bulk material flow. The results presented here suggest that the reconstruction of the high density of defect states associated with indentation fractures can take place in a unique parameter space different from that required for stress relief or bulk flow (Fig. 5). This implies that the annealing processes required to substantially increase the optical damage threshold of small surface imperfections on fused silica can be achieved through a judicious combination of temperature and annealing time. Such a method could, in principle, be used to treat any optic of arbitrary size, provided heating and cooling is spatially uniform, such that distortions in optical figures that might compromise the optical properties of the component are avoided.

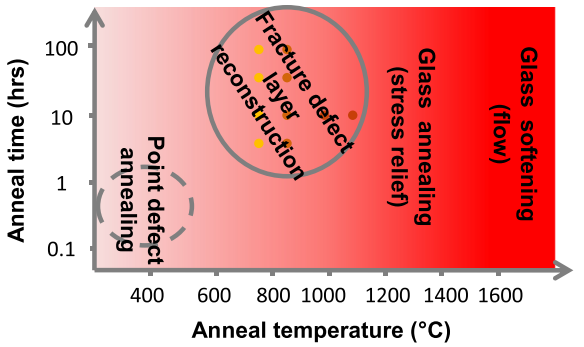

Fig. 5 Schematic representation of temperature dependent processes in fused silica.

As the annealing temperature approaches that required to release mechanical stress (approximately 1200°C), one begins to observe the partial healing or closing the smaller (micrometer or less) fractures whose surfaces are in close proximity to one another (Fig. 6). Similar behavior was not

Table 1 Activation energy of the thermal reconstruction of fracture defects.

Indent load (N)	F_{room} (J/cm^2)	F_0	Activation energy (kJ/mol)
0.5	5.5	91.9	9.7
2	4.8	370	26.0
5	3.4	669	42.3
10	1.0	703	53.7

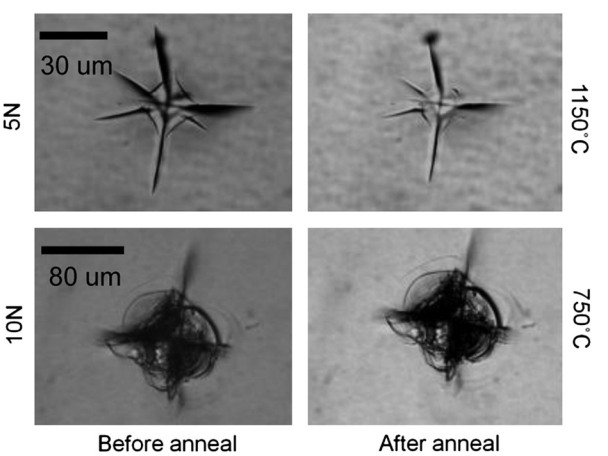

Fig. 6 Microscopy images of morphological changes exhibited by indentation fractures prior to and following thermal annealing.

observed on larger fractures. This could be expected[22] as the temperature approaches the glass transition temperature since the characteristic time to heal a feature of size L is $\mu L/\sigma$, where μ is the viscosity, and σ the surface tension. Since silica viscosity is an exponential function of temperature, the size of features that can be closed is expected to vary exponentially with annealing temperature.

This suggests that the proximity of the two surfaces may be of importance during the thermally mitigated reconstruction of the defect structure that underlies optical damage. Alternately, the thermally driven increase in laser damage threshold reported here may be the result of strictly a surface diffusion phenomenon, which does not require the close proximity of a mating surface. To explore this question we used the direct cleavage double compression (DCDC) method to grow a matching pair of isolated fracture surfaces.[9,23] Surprisingly, unlike indentation fractures, very little FPL signal was observed on the fracture surfaces produced using the DCDC technique. The high damage threshold of the fractures produced using the DCDC method was similar to that of a fracture-free, polished surface. The fracture surfaces created during the DCDC experiment are produced under pure tensile stress conditions at or near the critical stress intensity. Fractures formed during indentation and during laser damage are presumably created much more violently and under conditions of much higher stress intensity. These differences likely result in a significant difference in the population of electronic defects states remaining on surfaces following macroscopic fracture. Further study is presently underway to better understand both the origin and population of defects associated with fracture surfaces, and to develop more effective strategies to improve optics performance.

5 Conclusion

In the absence of photoactive impurities in the polishing layer, thermal processes, even at temperatures well below that required to relive mechanical stresses, reduce FPL defects and improve the ultraviolet laser damage threshold of fractures on fused silica surfaces. We attribute this behavior to a reduction in the population of electronic defects states formed on fracture surfaces during violent processes, such as indentation. It remains unclear if the reduction in defect population, as evidenced by both the observed reduction on FPL intensity and increase in local damage threshold, is the result of surface diffusion or requires the presence of a mating surface in close proximity.

Acknowledgments

This work performed under the auspices of the U.S. Department of Energy by Lawrence Livermore National Laboratory under Contract DE-AC52-07NA27344.

References

1. T. C. Sangster et al., "Overview of inertial fusion research in the United States," *Nucl. Fusion* **47**(10), S686–S695 (2007).
2. J. Caird et al., "Nd:glass laser design for laser ICF fission energy (LIFE)," *Fusion Sci. Technol.* **56**(2), 607–617 (2009).
3. J. Lindl, "Development of the indirect-drive approach to inertial confinement fusion and the target physics basis for ignition and gain," *Phys. Plasma* **2**(11), 3933–4024 (1995).
4. J. Nuckolls et al., "Laser compression of matter to super-high densities —thermonuclear (ctr) applications," *Nature* **239**(5368), 139 (1972).
5. S. C. Jones et al., "Recent progress on laser-induced modifications and intrinsic bulk damage of wide-gap optical-materials," *Opt. Eng.* **28**(10), 1039–1068 (1989).
6. B. C. Stuart et al., "Optical ablation by high-power short-pulse lasers," *J. Opt. Soc. Am. B* **13**(2), 459–468 (1996).
7. J. Bude et al., "The effect of lattice temperature on surface damage in fused silica optics," *Proc. SPIE*, **6720**, 672009 (2008).
8. T. A. Laurence et al., "Metallic-like photoluminescence and absorption in fused silica surface flaws," *Appl. Phys. Lett.* **94**(15), 151114 (2009).
9. P. E. Miller et al., "Fracture incuded sub-band gap absorption as a precursor to optical damage on fused silica surfaces," *Opt. Lett.* **35**(16), 2702–2704 (2010).
10. B. Lawn and R. Wilshaw, "Indentation fracture—principles and applications," *J. Mater. Sci.* **10**(6), 1049–1081 (1975).
11. G. Pacchioni, L. Skuja, and D. L. Griscom, *Defects in SiO_2 and Related Dielectrics: Science and Technology*, Springer, Kluwer, Dordrecht (2000).
12. L. Skuja, "The origin of the intrinsic 1.9 Ev luminescence band in glassy SiO_2," *J. Non-Cryst. Solids* **179**, 51–69 (1994).
13. L. Skuja, "Optically active oxygen-deficiency-related centers in amorphous silicon dioxide," *J. Non-Cryst. Solids* **239**(1–3), 16–48 (1998).
14. J. F. Latkowski et al., "Fused silica final optics for inertial fusion energy: radiation studies and system-level analysis," *Fusion Sci. Technol.* **43**(4), 540–558 (2003).
15. H. B. Sun et al., "Generation and recombination of defects in vitreous silica induced by irradiation with a near-infrared femtosecond laser," *J. Phys. Chem. B* **104**(15), 3450–3455 (2000).
16. C. Janssen, "Specimen for fracture mechanics studies on glass," *Rev. Phys. Appl.* **12**(5), 803–803 (1977).
17. R. L. Smith and G. E. Sandland, "An accurate method of determining the hardness of metals, with particular reference to those of a high degree of hardness," *Proc. Inst. Mech. Eng.* **1**, 623–641 (1922).
18. P. E. Miller et al., "Laser damage precursors in fused silica," *Proc. SPIE* **7504**, 75040X (2009).
19. T. A. Laurence et al., "Ultrafast photoluminescence as a diagnostic for laser damage initiation" *Proc. SPIE* **7504**, 750416 (2009).
20. J. Hue et al., "R-on-1 automatic mapping: a new tool for laser damage testing," *Proc. SPIE* **2714**, 90–100 (1996).
21. T. I. Suratwala et al., "HF-based etching processes for improving laser damage resistance of fused silica optical surfaces," *J. Am. Ceram. Soc.* **94**(2), 416–428 (2011).
22. M. D. Feit and A. M. Rubenchik, "Mechanisms of CO_2 laser mitigation of laser damage growth in fused silica," *Proc. SPIE* **4932**, 91–102 (2002).
23. S. N. Crichton et al., "Subcritical crack growth in a phosphate laser glass," *J. Am. Ceram. Soc.* **82**(11), 3097–3104 (1999)

Biographies and photographs of the authors are not available.